Bioorganic & Medicinal Chemistry Letters 20 (2010) 1004–1007

Contents lists available at ScienceDirect

Bioorganic & Medicinal Chemistry Letters

journal homepage: www.elsevier.com/locate/bmcl

Structure-based drug design of tricyclic 8*H*-indeno[1,2-*d*][1,3]thiazoles as potent FBPase inhibitors

Tomoharu Tsukada [a], Mizuki Takahashi [b], Toshiyasu Takemoto [a], Osamu Kanno [a], Takahiro Yamane [a], Sayako Kawamura [b], Takahide Nishi [a,*]

[a] *Medicinal Chemistry Research Laboratories I, Daiichi Sankyo Co., Ltd, 1-2-58 Hiromachi, Shinagawa-ku, Tokyo 140-8710, Japan*
[b] *Exploratory Research Laboratories I, Daiichi Sankyo Co., Ltd, 1-16-13 Kitakasai, Edogawa-ku, Tokyo 134-8630, Japan*

ARTICLE INFO

Article history:
Received 22 October 2009
Revised 8 December 2009
Accepted 11 December 2009
Available online 21 December 2009

Keywords:
FBPase
Diabetes

ABSTRACT

With the goal of improving metabolic stability and further enhancing FBPase inhibitory activity, a series of tricyclic 8*H*-indeno[1,2-*d*][1,3]thiazoles was designed and synthesized with the aid of structure-based drug design. Extensive SAR studies led to the discovery of **19a** with an IC_{50} value of 1 nM against human FBPase. X-ray crystallographic studies revealed that high affinity of **19a** was due to the hydrophobic interaction arising from better shape complementarity and to the hydrogen bonding network involving the side chain on the tricyclic scaffold.

Fructose-1,6-bisphosphatase (FBPase) is one of the enzymes involved in the rate-limiting steps of hepatic gluconeogenesis, and catalyzes the hydrolysis of fructose-1,6-bisphosphate to fructose-6-phosphate.[1] FBPase inhibitors would lower blood glucose levels by reducing hepatic glucose output and are expected to be a novel class of drugs for the treatment of Type 2 diabetes mellitus. Several classes of small-molecule inhibitors of FBPase have been reported.[2–6] Among them, AMP mimetic MB05032 (**1**) exhibited high inhibitory activity. A prodrug of MB05032 (CS-917, **2**) lowered blood glucose levels in animal models and was entered into clinical development (Fig. 1).[7]

In the previous Letter, we described the design and synthesis of tricyclic thiazoles as FBPase inhibitors, and a series of SAR studies led to the identification of phosphate **3** exhibiting potent FBPase inhibitory activity (IC_{50} = 13 nM) (Fig. 2).[8] In addition, we reported the finding of non-hydrolyzable difluoromethylenephosphonate **4** which also showed high inhibitory activity (IC_{50} = 47 nM).[8] However, subsequent attempts to evaluate the inhibitory effect on cellular glucose production of **4** and corresponding prodrug compound **5** were not successful. These results were rationalized by considering the metabolism of the amino group on the tricyclic scaffold. In fact, the amino groups of these compounds were readily metabolized by *N*-acetyltransferases. In order to improve metabolic stability and to enhance FBPase inhibitory activity, we turned our attention to further modification of our tricyclic-based inhibitors with the aid of structure-based drug design.

In order to address the problem of the metabolically unstable amino group on tricyclic scaffolds, we examined the conversion of the amino group. Our previous SAR studies led to the identification of compound **6** which possessed the non-hydrolyzable oxymethylphosphonate moiety and showed moderate FBPase inhibitory activity (IC_{50} = 124 nM).[8] Therefore, we selected compound **6** for the modification of the amino group. An X-ray crystal

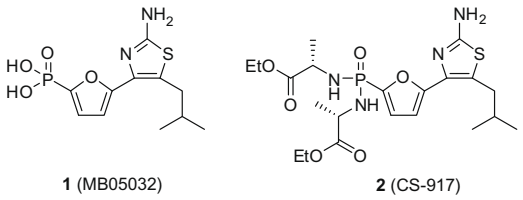

1 (MB05032) **2** (CS-917)

Figure 1. Structures of known FBPase inhibitors.

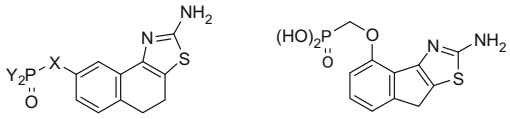

3 X = O, Y = OH
4 X = CF_2, Y = OH
5 X = CF_2, Y = (*S*)-NHCH(Me)CO_2Et

6

Figure 2. Structures of tricyclic-based FBPase inhibitors.

* Corresponding author. Tel.: +81 3 3492 3131; fax: +81 3 5436 8563.
E-mail address: nishi.takahide.xw@daiichisankyo.co.jp (T. Nishi).

0960-894X/$ - see front matter © 2010 Elsevier Ltd. All rights reserved.
doi:10.1016/j.bmcl.2009.12.056

structure of human liver FBPase in complex with **6** suggested the possibility of removing the amino group (Fig. 3).[9] The complex structure suggested that the amino group of **6** interacted with a carbonyl oxygen of Val17 and a side chain oxygen (Oγ) of Thr31 through hydrogen-bonding interaction. On the other hand, the amino group was located near the hydrophobic surface area formed by hydrophobic residues of Val17, Leu34, and Met177. In addition, the carbonyl oxygen of Val17 and Oγ of Thr31 forms hydrogen bonds to backbone amide nitrogen of Gly21 and a water molecule, respectively, suggesting that the interaction to the amino group of compound **6** might not be crucial in retaining the protein structure to the inhibited conformation. Based on these observations, we hypothesized that hydrophobic interaction instead of the interaction through the amino group might be beneficial to obtain high affinity. This led us to focus on replacing the amino group of compound **6** with other hydrophobic substituents.

Tricyclic thiazoles without amino group were synthesized according to Scheme 1. Commercially available 7-hydroxy-1-indanone **7** was converted to diethyl phosphonate **8**. Bromination of **8** followed by cyclization with thioacetamide, thioformamide (in situ generation), and thiourea gave 2-methythiazole (**9a**), thiazole (**9b**), and 2-aminothiazole (**9c**) intermediates, respectively. The hydrolysis of intermediates **9a**,**b** afforded the desired compounds **10a**,**b**. In addition, 2-halogen thiazole analogues **11a**,**b** were prepared from **9c** by a Sandmeyer reaction followed by hydrolysis.

The inhibitory activities of the compounds with the modification of the amino group against human liver FBPase are summarized in Table 1.[10] Replacement of the amino group of **6** with hydrophobic substituent such as a methyl group (**10a**) led to a substantial loss of activity (IC_{50} = 995 nM). Similarly, replacement with halogen groups (**11a**, **11b**) resulted in a considerable loss of activity (IC_{50} = 908, 772 nM, respectively). These results were presumably due to the loss of hydrogen-bonding interaction between the amino group and FBPase. In contrast, to our surprise, 10-fold increase in activity (IC_{50} = 12 nM) was achieved by removing the amino group of **6** (**10b**), and the activity of **10b** was almost equal to that of MB05032.

In order to obtain insights into the binding mode of desamino compound **10b**, an X-ray crystal structure of human liver FBPase in complex with **10b** was determined and was compared to that of corresponding amino compound **6** (Fig. 4). The phosphonate group of **10b** occupies the same position as that of **6**, and interacts

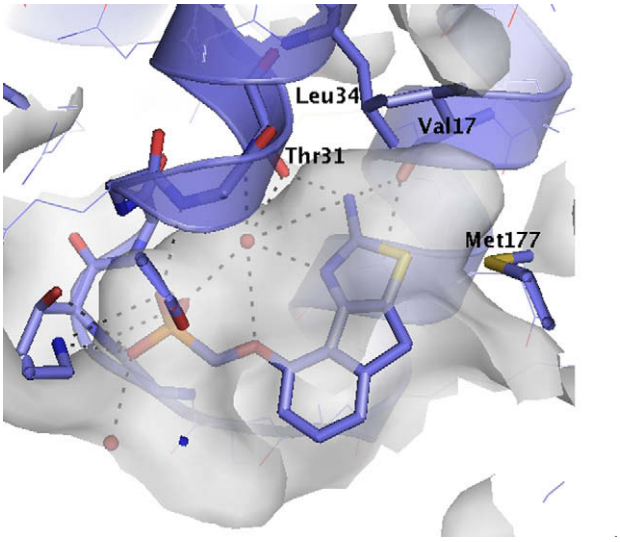

Figure 3. X-ray crystal structure of human liver FBPase in complex with **6**.

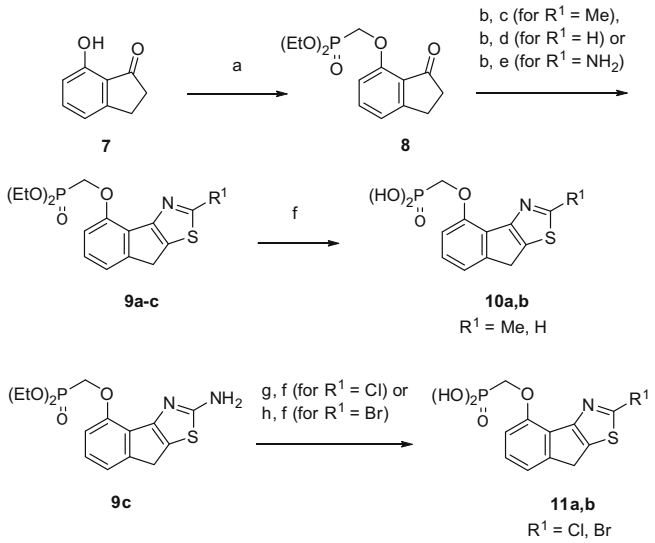

Scheme 1. Synthesis of compounds **10**–**11**. Reagents and conditions: (a) $(EtO)_2P(O)CH_2OTs$, K_2CO_3, DMF, 80 °C, 70%; (b) $CuBr_2$, EtOH, 60 °C, 98%; (c) thioacetamide, DMF, 50 °C, 41%; (d) P_2S_5, $HCONH_2$, THF, reflux, 66%; (e) thiourea, NaOAc, EtOH, reflux, 46%; (f) TMSBr, CH_2Cl_2, 90–98%; (g) ^tBuONO, $CuCl_2$, MeCN, 33%; (h) ^tBuONO, $CuBr_2$, MeCN, 44%.

Table 1
FBPase inhibitory activity of compounds **10**–**11**

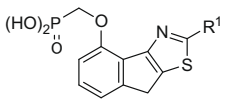

Compound	R^1	IC_{50}[a] (nM)
MB05032		10
6	NH_2	124
10a	Me	995
11a	Cl	908
11b	Br	772
10b	H	12

[a] Inhibition of human liver FBPase.

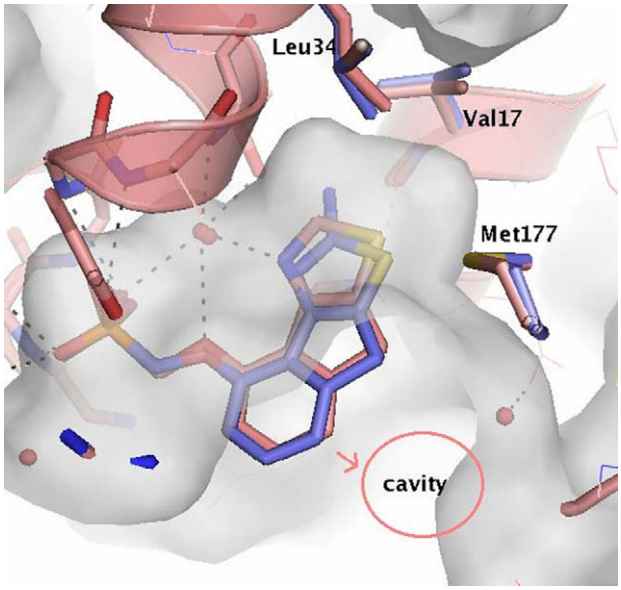

Figure 4. X-ray crystal structure of human liver FBPase in complex with **10b**. (Overlay of **6**. Compound **6** and residues Leu34, Val17 and Met177 in complex with **6** are colored in blue.)

with the backbone amides and the side chains of FBPase in a similar way to **6**. In contrast, when they were superimposed, a small but distinct shift of the tricyclic scaffold was observed. The tricyclic scaffold of **10b** shifts to the hydrophobic surface area formed by hydrophobic residues of Val17, Leu34, and Met177. In addition, side chains of these residues appear to be moved slightly to improve the shape complementarity to **10b**. The shift of tricyclic scaffold of **10b** and induced fit of hydrophobic side chains led to the formation of the hydrophobic interaction between the hydrophobic surface area and the thiazole ring of the tricyclic scaffold. This hydrophobic interaction reinforced by better shape complementarity would compensate for the loss of the hydrogen-bonding interactions between the amino group and FBPase. In other words, the amino group of **6** contributes not only to hydrogen-bonding interaction but also to steric reputation to some extent.

Moreover, the X-ray co-crystal structure of **10b** provided important clues for further development. The complex structure suggested that there was a cavity in the direction of the 7-position of tricyclic scaffold (*p*-position of oxymethylphosphonate moiety) and also showed that there were some water molecules in this space. We expected higher affinity might be obtained by introducing the side chains which occupied the cavity, especially the side chains with the potential to interact to the water molecules. Based on these considerations, we focused our attention on introducing side chains mainly to the 7-position of tricyclic scaffold to further enhance its FBPase inhibitory activity.

Tricyclic thiazoles with side chains were synthesized according to Scheme 2. The compounds with alkyl or halogen side chains (**15a–f**) were prepared from corresponding phenols **12a–g**. Acylation of **12a–g** followed by a Fries rearrangement and the introduction of a diethyl phosphonate unit resulted in **13a–g**, which were transformed into intermediates **14a–g** and desired compounds **15a–f** by the subsequent steps already described in Scheme 1. The compounds with aromatic side chain (**16a–e**) were obtained from intermediate **14g** by Suzuki couplings with corresponding boronic acids/esters followed by hydrolysis. The compounds with amide side chain (**19a**,**b**) were obtained from intermediate **13g**. CO insertion of **13g** followed by a transesterification reaction resulted in allyl ester **17**, which was transformed into carboxylic acid **18** via bromination followed by cyclization and deesterification. Amidation of **18** with corresponding amines and subsequent hydrolysis afforded desired compounds **19a**,**b**.

The inhibitory activities of the compounds containing the side chains are summarized in Table 2. The attempts to occupy the cavity with hydrophobic substituents such as alkyl groups and halogen groups were slightly effective to ineffective in increasing inhibitory activity. The insertion of Me (**15a**), Et (**15b**), F (**15c**), and Cl (**15d**) at 7-position showed similar inhibitory activities (IC_{50} = 8, 11, 15, 8 nM, respectively) to lead compound **10b**. With disubstitution, 6,7-disubstitution such as 6,7-di Me (**15e**) and 6,7-di F (**15f**) were tolerated (IC_{50} = 10, 9 nM, respectively). The efforts to incorporate aromatic ring at the 7-position led to a range of results, including detrimental effects with Ph (**16a**) and 2-Py (**16b**) (IC_{50} = 28, 40 nM, respectively), minor effects with 3-Py (**16c**) and 4-Py (**16d**) (IC_{50} = 9, 9 nM, respectively), and fourfold boost in potency with 3,5-pyrimidine (**16e**) (IC_{50} = 3 nM). These results suggested that the incorporation of a hydrogen bond acceptor into its proper location was beneficial to increase inhibitory activity, whereas only occupying the cavity was relatively ineffective. On the basis of these findings, we introduced other hydrogen bond acceptor such as a carbonyl group. The efforts to introduce amide groups (**19a**, **19b**) provided a major boost in inhibitory activity (IC_{50} = 1, 2 nM, respectively), and **19a** was over 10-fold more potent than lead compound **10b**.

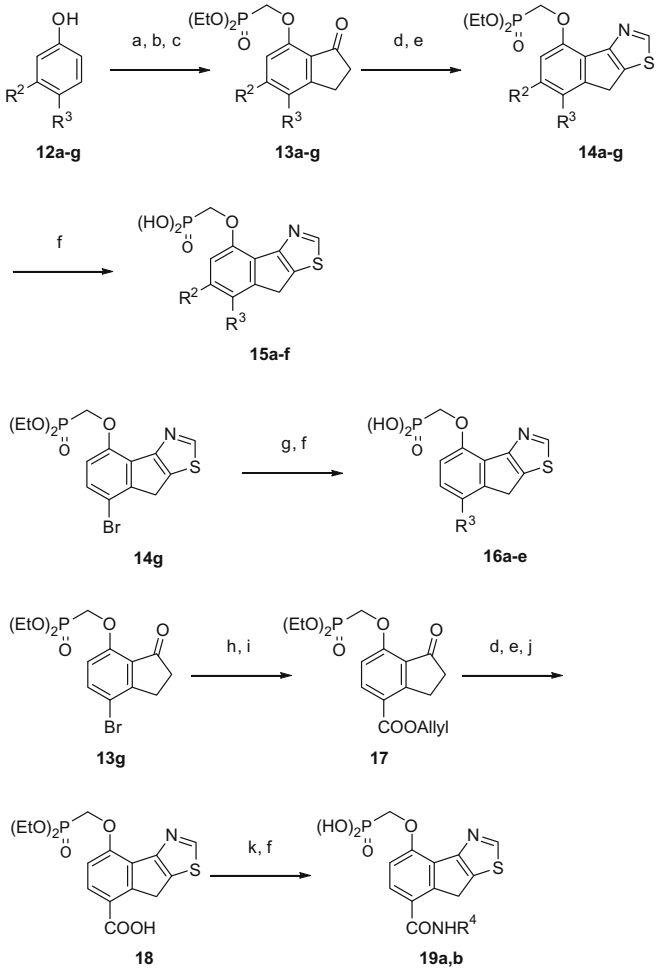

Scheme 2. Synthesis of compounds **15**–**19**. Reagents and conditions: (a) $ClCH_2CH_2COCl$, pyridine, CH_2Cl_2, 56–98%; (b) $AlCl_3$, 180 °C, 32–90%; (c) $(EtO)_2P(O)$-CH_2OTs, K_2CO_3, DMF, 80 °C, 57–98%; (d) $CuBr_2$, EtOH, 60 °C, 90–98%; (e) P_2S_5, $HCONH_2$, THF, reflux, 45–71%; (f) TMSBr, CH_2Cl_2, 66–98%; (g) boronic acid/ester, $Pd(PPh_3)_4$, Na_2CO_3, EtOH–H_2O, reflux, 17–62%; (h) $Pd(OAc)_2$, dppp, CO, Et_3N, $TMSCH_2CH_2OH$, DMF, 70 °C, 52%; (i) TBAF, allyl bromide, Et_3N, 93%; (j) $Pd(PPh_3)_4$, pyrrolidine, MeCN, 79%; (k) amine, WSC, HOBt, DMF, 47–73%.

Table 2
FBPase inhibitory activity of compounds **15**–**19**

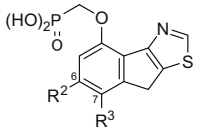

Compound	R^2	R^3	IC_{50}[a] (nM)
10b	H	H	12
15a	H	Me	8
15b	H	Et	11
15c	H	F	15
15d	H	Cl	8
15e	Me	Me	10
15f	F	F	9
16a	H	Ph	28
16b	H	2-Py	40
16c	H	3-Py	9
16d	H	4-Py	9
16e	H	3,5-Pyrimidine	3
19a	H	$CONH_2$	1
19b	H	CONHMe	2

[a] Inhibition of human liver FBPase.

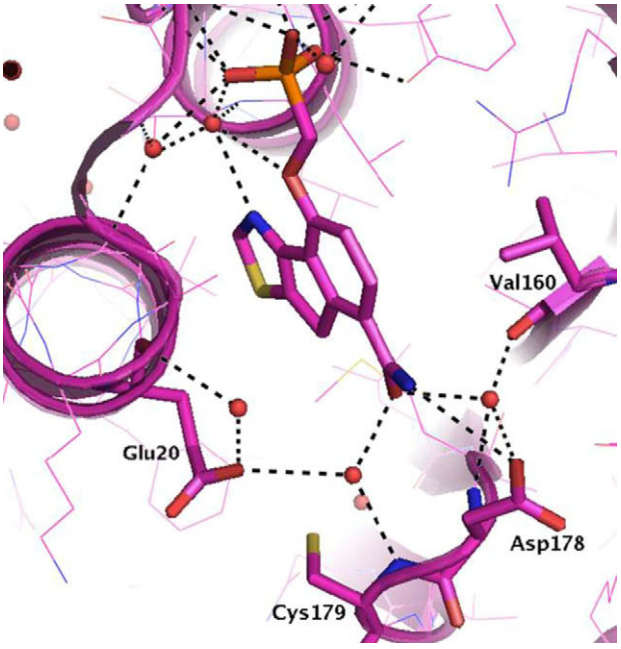

Figure 5. X-ray crystal structure of human liver FBPase in complex with **19a**.

In order to understand the determinants of high affinity of **19a** with amide side chain, an X-ray crystal structure of human liver FBPase in complex with **19a** was determined (Fig. 5). The position of phosphonate group and tricyclic scaffold of **19a** is similar to those of **10b** with no side chain, which suggests the formation of the hydrophobic interaction as in the case of **10b**. In addition, the amide side chain of **19a** makes hydrogen bonds with the side chain of Asp178 and two water molecules, as expected. One water molecule interacts with the backbone carbonyl oxygen of Val160, the backbone nitrogen (NH) of Asp178 and the side chain of Asp178, and the other water molecule interacts with the backbone nitrogen (NH) of Cys179 and the side chain of Glu20. As a result, the side chain of **19a** forms the hydrogen bonding network involving Val160, Asp178, Cys179, Glu20, and two water molecules. This hydrogen bonding network would contribute to increase affinity.

In summary, we further developed a series of tricyclic 8*H*-indeno[1,2-*d*][1,3]thiazoles as potent FBPase inhibitors with the aid of structure-based drug design. In order to enhance the metabolic stability, lead compound **6** was modified to desamino compound **10b** which showed 10-fold increase in inhibitory activity relative to **6**. The X-ray co-crystal structure of **10b** suggested that hydrophobic interaction would compensate for the loss of the hydrogen-bonding interactions through the amino group. Furthermore, introducing side chain with hydrogen bonding capability to **10b** led to the discovery of **19a** which exhibited over 10-fold increased activity compared to **10b**. This high affinity would be obtained by forming the hydrogen bonding network involving the side chain. The X-ray co-crystal structures of lead compounds (**6**, **10b**) provided us with the structural information which was beneficial to further developments, and these results demonstrated the usefulness of structure-based drug design. Further efforts on identifying various phosphonate prodrugs of the tricyclic 8*H*-indeno[1,2-*d*][1,3]thiazoles to investigate in vivo activity are underway.

Acknowledgments

We thank Professor Noriyoshi Sakabe of the Structural Biology Sakabe Project and Professor Soichi Wakatsuki of the Institute of Materials Structure Science for the use of the facilities at the Photon Factory.

References and notes

1. (a) Benkovic, S. J.; deMaine, M. M. *Adv. Enzymol. Relat. Areas Mol. Biol.* **1982**, *53*, 45; (b) Gidh-Jain, M.; Zhang, Y.; van Poelje, P. D.; Liang, J.-Y.; Huang, S.; Kim, J.; Elliott, J. T.; Erion, M. D.; Pilkis, S. J.; El-Maghrabi, M. R.; Lipscomb, W. N. *J. Biol. Chem.* **1994**, *269*, 27732; (c) Zhang, Y.; Liang, J.; Huang, S.; Lipscomb, W. N. *J. Mol. Biol.* **1994**, *244*, 609; (d) Iancu, C. V.; Mukund, S.; Fromm, H. J.; Honzatko, R. B. *J. Biol. Chem.* **2005**, *280*, 19737; (e) Pilkis, S. J.; El-Maghrabi, M. R.; Pilkis, J.; Claus, T. H. *J. Biol. Chem.* **1981**, *256*, 3619.
2. (a) Wright, S. W.; Hageman, D. L.; McClure, L. D.; Carlo, A. A.; Treadway, J. L.; Mathiowetz, A. M.; Withka, J. M.; Bauer, P. H. *Bioorg. Med. Chem. Lett.* **2001**, *11*, 17; (b) Wright, S. W.; Carlo, A. A.; Carty, M. D.; Danley, D. E.; Hageman, D. L.; Karam, G. A.; Levy, C. B.; Mansour, M. N.; Mathiowetz, A. M.; McClure, L. D.; Nestor, N. B.; McPherson, R. K.; Pandit, J.; Pustilnik, L. R.; Schulte, G. K.; Soeller, W. C.; Treadway, J. L.; Wang, I.-K.; Bauer, P. H. *J. Med. Chem.* **2002**, *45*, 3865.
3. Wright, S. W.; Carlo, A. A.; Danley, D. E.; Hageman, D. L.; Karam, G. A.; Mansour, M. N.; McClure, L. D.; Pandit, J.; Schulte, G. K.; Treadway, J. L.; Wang, I.-K.; Bauer, P. H. *Bioorg. Med. Chem. Lett.* **2003**, *13*, 2055.
4. Choe, J.-Y.; Nelson, S. W.; Arienti, K. L.; Axe, F. U.; Collins, T. L.; Jones, T. K.; Kimmich, R. D. A.; Newman, M. J.; Norvell, K.; Ripka, W. C.; Romano, S. J.; Short, K. M.; Slee, D. H.; Fromm, H. J.; Honzatko, R. B. *J. Biol. Chem.* **2003**, *278*, 51176.
5. (a) von Geldern, T. W.; Lai, C.; Gum, R. J.; Daly, M.; Sun, C.; Fry, E. H.; Abad-Zapatero, C. *Bioorg. Med. Chem. Lett.* **2006**, *16*, 1811; (b) Lai, C.; Gum, R. J.; Daly, M.; Fry, E. H.; Hutchins, C.; Abad-Zapatero, C.; von Geldern, T. W. *Bioorg. Med. Chem. Lett.* **2006**, *16*, 1807.
6. Hebeisen, P.; Kuhn, B.; Kohler, P.; Gubler, M.; Huber, W.; Kitas, E.; Schott, B.; Benz, J.; Joseph, C.; Ruf, A. *Bioorg. Med. Chem. Lett.* **2008**, *18*, 4708.
7. (a) Erion, M. D.; van Poelje, P. D.; Dang, Q.; Kasibhatla, S. R.; Potter, S. C.; Reddy, M. R.; Reddy, K. R.; Jiang, T.; Lipscomb, W. N. *Proc. Natl. Acad. Sci.* **2005**, *102*, 7970; (b) Erion, M. D.; Dang, Q.; Reddy, M. R.; Kasibhatla, S. R.; Huang, J.; Lipscomb, W. N.; van Poelje, P. D. *J. Am. Chem. Soc.* **2007**, *129*, 15480; (c) Dang, Q.; Rao Kasibhatla, S.; Reddy, K. R.; Jiang, T.; Reddy, M. R.; Potter, S. C.; Fujitaki, J. M.; van Poelje, P. D.; Huang, J.; Lipscomb, W. N.; Erion, M. D. *J. Am. Chem. Soc.* **2007**, *129*, 15491; (d) van Poelje, P. D.; Dang, Q.; Erion, M. D. *Drug Discovery Today* **2007**, *4*, 103.
8. Tsukada, T.; Takahashi, M.; Takemoto, T.; Kanno, O.; Yamane, T.; Kawamura, S.; Nishi, T. *Bioorg. Med. Chem. Lett.* **2009**, *19*, 5909.
9. The X-ray crystallographic study was accomplished according to the procedure described in Ref. 8. The FBPase-**6**, **10b**, **19a** cocrystals were diffracted to 2.45, 2.8, 2.25 Å in resolution, respectively. The coordinates and statistics are available from the PDB using accession codes 3kbz, 3kc0, and 3kc1, respectively.
10. Inhibition assays using recombinant human liver FBPase were performed according to the methods described in Ref. 7c.